

Sea water fugacity of CO₂ at the PIRATA mooring at 6°S, 10°W

By GAËLLE PARARD*, NATHALIE LEFÈVRE and JACQUELINE BOUTIN,
LOCEAN, Université Pierre et Marie Curie, 4 place Jussieu 75252 Paris cedex 05, France

(Manuscript received 22 December 2009; in final form 6 August 2010)

ABSTRACT

In order to better understand the variability of surface CO₂ in the Tropical Atlantic, a CARIOCA sensor has been installed on a PIRATA mooring at 6°S, 10°W in June 2006. The fugacity of CO₂ ($f\text{CO}_2$) is recorded hourly from 7 June 2006 to 30 October 2009 with two important data gaps. From July to September, an upwelling develops and a decrease in sea surface temperature (SST) is observed, associated with an $f\text{CO}_2$ increase. However, the highest $f\text{CO}_2$ is observed in October, after the upwelling season, due to the warming of surface waters. The region is a net source of CO₂ to the atmosphere of $2.10 \pm 0.69 \text{ mol m}^{-2} \text{ yr}^{-1}$ in 2007. The monthly flux is maximum ($3.21 \pm 0.8 \text{ mol m}^{-2} \text{ yr}^{-1}$) in November (averaged over 2006 and 2008). High frequency variability is observed throughout the time series but is particularly pronounced after the upwelling season. Biological and thermodynamic processes explain the diurnal variability. Dissolved inorganic carbon (DIC) is calculated from (alkalinity) TA and $f\text{CO}_2$ using an empirical TA–salinity relationship determined for the eastern equatorial Atlantic. Net community production (NCP) is calculated from DIC daily changes and ranges from 9 to 41 $\text{mmol m}^{-2} \text{ d}^{-1}$, which is consistent with previous measurements in this region.

1. Introduction

Ocean time series provide valuable information for monitoring and detecting climate changes and for understanding variability over a wide range of timescales in the physics, chemistry and biology of the ocean. However existing time series are still limited to a few sites for biogeochemical measurements (Send et al., 2009). Time series measurements have been proven to be very useful to monitor and interpret high frequency (from hourly) to long-term (up to decades) variability of sea surface carbon parameters. For instance, Bakker et al. (2001) evidenced significant diurnal cycles of the CO₂ fugacity ($f\text{CO}_2$) from a time series of a CARIOCA buoy drifting in the tropical Atlantic, that were driven either by the sea surface temperature (SST) or by the biological activity. More recently, Boutin and Merlivat (2009) took advantage of the latter property for estimating the net community production (NCP) from high frequency $f\text{CO}_2$ measurements when they appear to be dominated by biological activity. Concerning long-term variability, the three time series stations located in the northern subtropics [Bermuda Atlantic Time Series (BATS), European Station for Time Series in the

Ocean and the Canary Islands (ESTOC), and Hawaii Ocean Time Series (HOT)] indicate a rate of $f\text{CO}_2$ increase close to the atmospheric $f\text{CO}_2$ increase (Bindoff et al., 2007). In addition, air–sea CO₂ fluxes can be quantified and monitored. At ESTOC, González-Dávila et al. (2003) found a source of CO₂ for the atmosphere of $0.17 \text{ mol m}^{-2} \text{ yr}^{-1}$, much weaker than the source of $2.8 \pm 3.6 \text{ mol m}^{-2} \text{ yr}^{-1}$ from 1996 to 2000 given by Astor et al. (2005) for the CARIACO station (CARbon Retention In A Colored Ocean) located at 10.5°N, 64.67°W in the equatorial Atlantic. Both stations observe a very strong seasonal cycle (on the order of 100 μatm), but a much higher variability is observed at CARIACO due to the influence of the coastal upwelling.

Most of the time series require monthly visits with a ship so most of them are located relatively close to the coast (with depth lower than 500 m) for easy access (Fig. 1). With the development of autonomous biogeochemical sensors (Lefèvre et al., 1993; Byrne et al., 2009), time series of DIC (e.g. Sayles and Eck, 2009) or surface $f\text{CO}_2$ on fixed buoys (e.g. Copin-Montégut et al., 2004; Körtzinger et al., 2008; Lefèvre et al., 2008) or on drifting buoys (Bakker et al., 2001; Boutin and Merlivat, 2009; Merlivat et al., 2009) have started. In the Pacific, a CO₂ system using an infrared analyser (Chavez et al., 1997) has been installed on the Tropical Atmosphere Ocean (TAO) moored buoys and in coastal areas. It provides high-resolution time series measurements of surface ocean CO₂ partial pressure

*Corresponding author.

e-mail: gaplod@locean-ipsl.upmc.fr

DOI: 10.1111/j.1600-0889.2010.00503.x

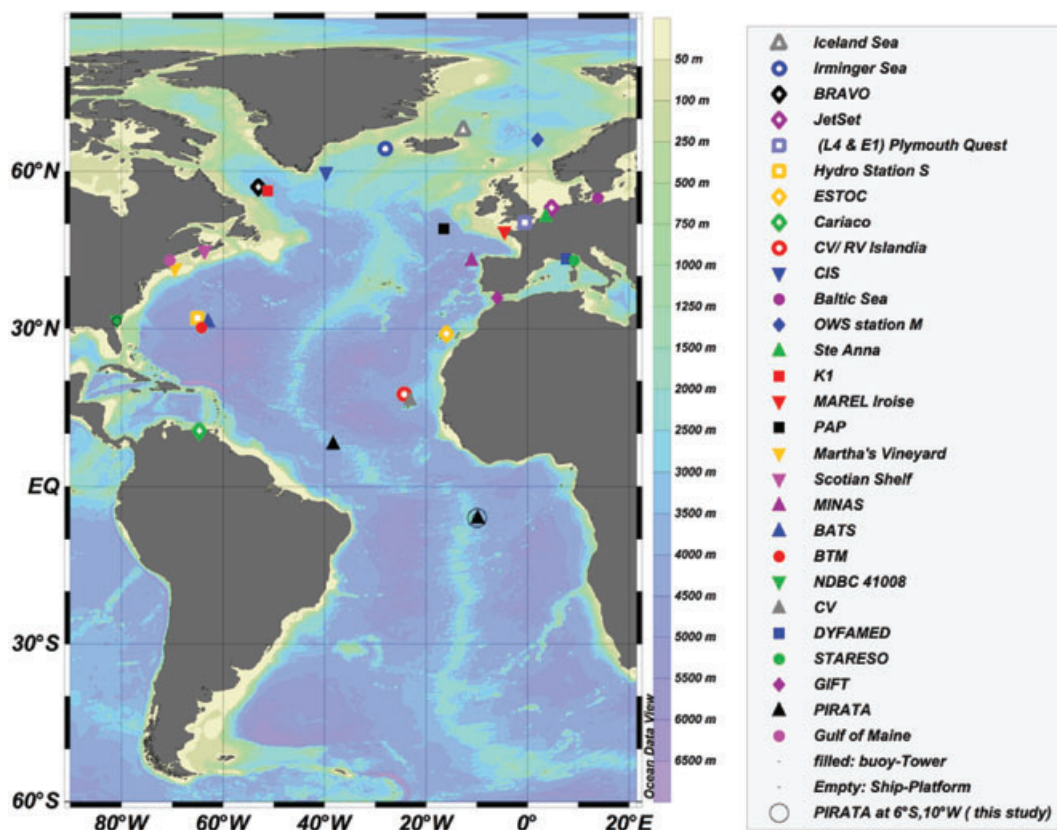


Fig. 1. Location of carbon time series stations in the Atlantic (according to IOCCP, October 2009, http://ioc3.unesco.org/ioccp/Hydrography/New_globalMap.html). The mooring 6°S, 10°W is indicated by a circle.

($p\text{CO}_2$). In coastal areas, the Santa Monica Bay Observatory mooring (SMBO) records hourly $p\text{CO}_2$. The recorded $p\text{CO}_2$ diurnal cycle shows a variability that can reach up to 150 μatm due to temperature changes and to biological activity (Leinweber et al., 2009). In comparison, the monitoring of the tropical Atlantic is well behind the tropical Pacific regarding CO_2 time series.

Our current knowledge of the carbon cycle in the tropical Atlantic comes mainly from the oceanographic cruises conducted in this region over the years. The characteristics of the $f\text{CO}_2$ distribution in this region are mainly related to the ocean circulation. The equatorial upwelling supplies CO_2 rich waters to the surface and leads to the high $f\text{CO}_2$ values reported during the FOCAL (Andrié et al., 1986), Cither (Oudot et al., 1995) and Polarstern cruises (Bakker et al., 1999). This makes the tropical Atlantic a source of CO_2 for the atmosphere. The climatology of Takahashi et al. (2009) estimates a source of 0.10 PgC yr^{-1} between 14°S and 14°N.

Recently, six oceanographic cruises, EGEE (for 'étude de la circulation océanique et de sa variabilité dans le golfe de Guinée'), conducted in the eastern equatorial Atlantic from 2005 to 2007 with two cruises a year, documented the variability of DIC and TA in the region 10°S–10°N, 10°W–10°E (Koffi et al.,

2010). South of about 2°N, the equatorial upwelling and the coastal upwelling off Angola merge to form a cold tongue that spreads westwards from June to September. The impact of this cold tongue was observed down to 6°S with high $f\text{CO}_2$ and low SST measured during the June 2006 cruise. During this cruise, the CO_2 sensor used in this paper was installed on a mooring at 6°S, 10°W and it is replaced every year. High precipitation associated with the seasonal migration of the Intertropical Convergence Zone (ITCZ) plays also an important role in the $f\text{CO}_2$ and salinity distribution of the equatorial Atlantic (Oudot et al., 1995). The north–south gradient of $f\text{CO}_2$ observed in the North Equatorial Counter Current (NECC) (e.g. Oudot et al., 1995) was also observed during the EGEE cruises in the Guinea Current and is considered as an extension of the NECC. In the western tropical Atlantic, the Amazon influence has also been observed (Ternon et al., 2000; Körtzinger, 2003; Lefèvre et al., 2010) and leads to lower $f\text{CO}_2$ compared to the surrounding high $f\text{CO}_2$ values.

This paper describes the variability of $f\text{CO}_2$ at 6°S, 10°W. SST and $f\text{CO}_2$ data were recorded hourly between 2006 and 2009 (from 7 June 2006 to 15 October 2007, from 16 September 2008 to 31 December 2008 and from 15 July to 30 October 2009). The processes affecting the CO_2 variation at

different timescales are investigated and the air–sea fluxes are estimated.

2. Methods

The ocean circulation in the tropical Atlantic is monitored by a network of 15 moored buoys, Prediction and Research Moored Array in the Tropical Atlantic (PIRATA). Each PIRATA mooring is equipped with a SEABIRD sensor for measuring temperature every 10 min and hourly salinity from the surface to respectively 500 and 120 m (20, 40, 80, 120, 150, 200, 300 and 500 m). Other parameters, such as wind speed at 4 m height, air temperature, precipitation and short-wave radiation are also measured at high frequency (Bourlès et al., 2008). The data are available on the PIRATA website (<http://www.pmel.noaa.gov/pirata>) where daily means are provided in near-real time using Argos transmission.

In June 2006, a CARIOCA $f\text{CO}_2$ sensor was added on the PIRATA mooring at 6°S, 10°W (Lefèvre et al., 2008). CARIOCA is an autonomous sensor using a colorimetric method to measure $f\text{CO}_2$ (Lefèvre et al., 1993; Hood and Merlivat, 2001). The seawater intake is located at 1.5 m below the surface. A copper pipe has been used to supply seawater to the sensor in order to prevent biofouling. The sensor gives $f\text{CO}_2$ with an accuracy of $\pm 3 \mu\text{atm}$ and a precision of $\pm 1 \mu\text{atm}$ (Bates et al., 2000). The $f\text{CO}_2$ data recorded in 2006 have been reported by Lefèvre et al. (2008).

Hourly $f\text{CO}_2$ and SST measurements are sent in real time by Argos and the sensor is replaced every year. The first sensor was installed on 6 June 2006, and was replaced successively on 28 June 2007 and 16 September 2008. The sensor currently on the mooring was installed on 10 July 2009. Failures occurred sometimes so that several gaps exist in the data time series. Each CO_2 sensor is calibrated in the laboratory with a CO_2 system based on infrared detection (using a Licor 6262) before deployment and after recovery. Each sensor includes two bags of dye. A small volume of dye is pumped to make the $f\text{CO}_2$ measurement and is sent to a waste bag. When the sensor is recovered, the calibration is made with the remaining dye in the laboratory. In 2006, during the installation of the first sensor, a comparison between the shipboard infrared CO_2 system and the CARIOCA sensor showed a very good agreement between the two techniques (Lefèvre et al., 2008). After recovery, the sensor was calibrated and no correction of the $f\text{CO}_2$ data was necessary for the 2006 data. In 2007 and 2008 the sensor drifted and this was confirmed by the calibration after recovery. The start of the drift could also be detected by recording the absorbance of the dye at different wavelengths. Data were disregarded when the sensor started drifting. The sensor installed in July 2009 was not recovered yet, so the data after the 10 July 2009 are considered as preliminary. However, no drift was detected.

Using the SSS recorded at the mooring with the highest available resolution (hourly in 2006 and 2007; daily in 2008 and

2009), TA was calculated with the relationship determined by Koffi et al. (2010).

$$\text{TA} = 65.222 \times \text{SSS} + 2.50 \quad r^2 = 0.97. \quad (1)$$

The standard error on the predicted alkalinity is $\pm 7.2 \mu\text{mol kg}^{-1}$. This relationship is valid for SSS ranging from 32 to 37.

DIC, expressed in $\mu\text{mol kg}^{-1}$, is calculated from $f\text{CO}_2$, TA, SST and SSS using the dissociation constants of Merbach et al. (1973) refitted by Dickson and Millero (1987). The error on TA using eq. (1), the error on dissociation constants and the accuracy of the $f\text{CO}_2$ sensor of $\pm 3 \mu\text{atm}$ leads to an error in calculated DIC of $8.7 \mu\text{mol kg}^{-1}$. Direct DIC measurements are available from the EGEE cruises (Koffi et al., 2010). The calculated DIC of $213.8 \mu\text{mol kg}^{-1}$, corresponding to the average of DIC over the 7–8 June 2006, is in good agreement with the DIC of $210.5 \pm 2 \mu\text{mol kg}^{-1}$ measured at 6°S, 10°W (6 June 2006) during the EGEE 3 cruise. DIC was also measured in November 2006 and at the end of June 2007. The measurements of $260.0 \pm 2 \mu\text{mol kg}^{-1}$ (23 November 2006) and $228.3 \pm 2 \mu\text{mol kg}^{-1}$ (28 June 2007) compare well with the calculated values of $267.5 \pm 8.7 \mu\text{mol kg}^{-1}$ and $227.1 \pm 8.7 \mu\text{mol kg}^{-1}$ averaged over the 28–29 June 2006 and 23–24 November 2006, respectively.

The daily air–sea CO_2 flux (F_{CO_2}), expressed in $\text{mmol m}^{-2}\text{d}^{-1}$, is computed using the daily mean of the wind speed converted to 10 m height. The flux is calculated as follows:

$$F_{\text{CO}_2} = k_{\text{CO}_2} \alpha (f\text{CO}_2 - f\text{CO}_{2\text{atm}}), \quad (2)$$

where α is the solubility of CO_2 (Weiss, 1974), k_{CO_2} is the gas transfer velocity (Sweeney et al., 2007), and $f\text{CO}_2$ is the surface $f\text{CO}_2$ recorded at the mooring. Atmospheric $f\text{CO}_2$ ($f\text{CO}_{2\text{atm}}$) is computed from the water vapour pressure (Weiss and Price, 1980), the atmospheric pressure measured at the mooring and the weekly atmospheric molar fraction ($\times\text{CO}_2$). $\times\text{CO}_2$ value in dry air is provided by Globalview- CO_2 at the Ascension island (7.92°S, 14.42°W) from 2006 to 2009 (<ftp.cml.noaa.gov>, path:ccg/co2/GLOBALVIEW). Between 2006 and 2009, monthly $f\text{CO}_{2\text{atm}}$ varies from 356 to 369 μatm .

Array for Real-Time Geostrophic Oceanography (ARGO) float profiles obtained from the Coriolis Data Assembly Center have been collocated with the buoy at $\pm 2^\circ$ in latitude and longitude and ± 5 d. The temperature profiles are used to estimate the depth of the mixed layer using criteria following $\Delta T \geq 0.2^\circ\text{C}$ by Boyer-Montegut et al. (2004).

In order to examine the oceanic conditions around the mooring, SST maps derived from TMI [TRMM Microwave Imager (Tropical Rainfall Measuring Mission)] with a 25 km, 3-d resolution have been used (ftp.ssmi.com/tmi/bmaps_v04).

We often observe variability at short timescale superimposed to seasonal variability. A Morlet wavelet analysis (Torrence and Compo, 1998) is used to characterize the variability over the whole time series. In order to remove low frequency variability,

the data have been filtered at 5 d. Two parameters are obtained with the Morlet wavelet: the mean power of the global spectrum that indicates the dominant frequencies of the $f\text{CO}_2$ time series and the modulus of the wavelet transform that indicates how the dominant frequencies vary in time.

3. Results

3.1. Hydrographic situation

The mooring at 6°S, 10°W is located in the South Equatorial Current (SEC) that flows westward and extends from the surface to 100 m. This current covers a large range of latitudes from approximately 2°N to 15–25°S depending on the longitudinal location and time of year. During the upwelling season, between June and September, the mooring at 6°S, 10°W is affected by the propagation of the cold tongue. This cold tongue, formed by the merging of the equatorial upwelling and the coastal upwelling off the coast of Angola, is advected westward by the SEC. The equatorial upwelling, centred around 2°S, occurs between June and September. It brings water from the Equatorial UnderCurrent (EUC) to the surface, which significantly cools the surface layer, by about 5°C (Hazeleger et al., 2003). Thus, the occurrence of the equatorial upwelling is evidenced by cooler (<25°C) and saltier (>36) waters (Voituriez and Herbland, 1979) than the tropical surface waters (Bakun, 1978) that are characterized by temperature of about 27°C (Stramma and Schott, 1999).

In order to examine the timing and the impact of the cold tongue at the mooring, TMI SST are plotted between 8°S

and 2°N along 10°W (Fig. 2). A cooler period with a mean 2006–2009 temperature of $24.23 \pm 0.37^\circ\text{C}$ occurs from June to September. A warm period is observed between February and May with a surface temperature of $28.05 \pm 0.20^\circ\text{C}$ averaged between 2006 and 2009 over the region 4°N–10°S at 10°W. The equatorial upwelling is centred on 1 to 2°S, where we observed the coldest SST (Fig. 2). SSTs below 23°C are observed during the 15 July–15 September period, which corresponds to the main upwelling period. However, there is significant year-to-year variability in the strength of the equatorial upwelling. For instance, the mean SST values between June and September are similar in 2006 ($23.58 \pm 0.1^\circ\text{C}$) and 2007 ($23.66 \pm 0.06^\circ\text{C}$), whereas the mean SST is slightly higher in 2008 ($23.95 \pm 0.1^\circ\text{C}$) and lower in 2009 ($22.98 \pm 0.4^\circ\text{C}$). The coldest month is always observed in 2009. This suggests that the upwelling in 2009 is the strongest. In 2008, the equatorial upwelling is on average weaker than the others, although in July ($23.50 \pm 0.09^\circ\text{C}$) and in September ($23.26 \pm 0.07^\circ\text{C}$), the SST is lower than in 2006 and 2007. The SST in 2008 has a minimum in September while the SST minimum is observed in August for the other years. At the mooring, the propagation of the cold tongue, formed by the equatorial and coastal upwellings, affects the SST.

Near the mooring, between 5°S and 7°S at 10°W, the SST, averaged over the June–September period, is $24.97 \pm 0.5^\circ\text{C}$ in 2009. At the equator, the coldest SSTs are observed in 2009 whereas, at the mooring, although the mean SST is slightly lower than in 2006 ($25.18 \pm 0.07^\circ\text{C}$) and in 2007 ($25.15 \pm 0.02^\circ\text{C}$), the year 2009 is not significantly colder than 2006 and 2007 given the standard deviation of 0.5°C. However, in 2008,

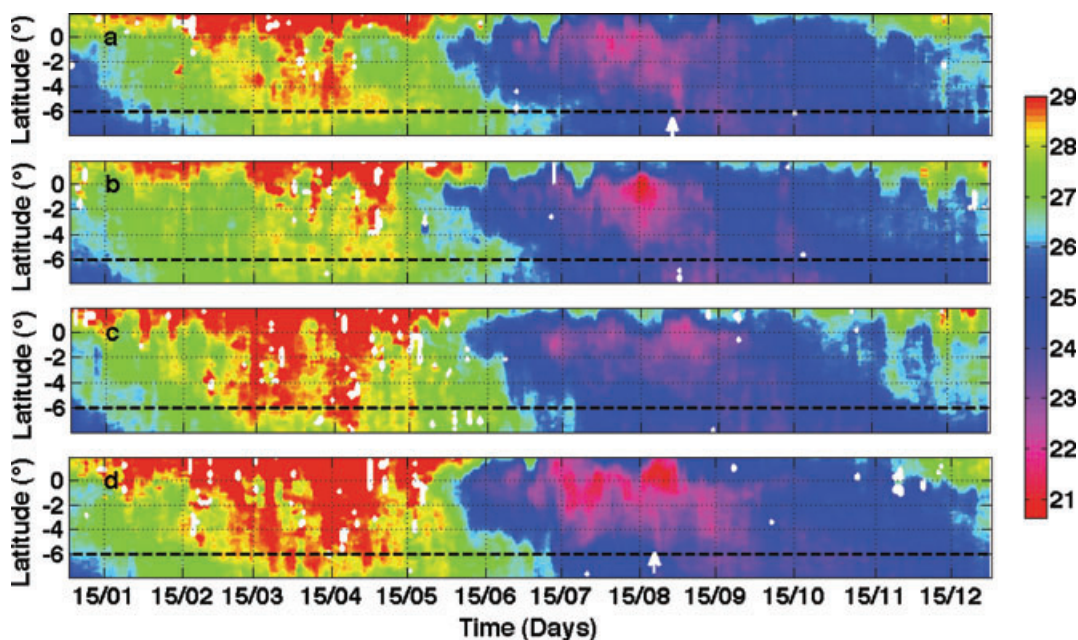


Fig. 2. Hovmöller latitude-time diagrams of TMI SST ($^\circ\text{C}$) along 10°W (a) in 2006 (b) in 2007 (c) 2008 (d) 2009. The dashed line corresponds to the latitude of 6°S. The arrow in (a) indicates the 27 August 2006 and in (d) 25 August 2009. Missing values are indicated in white.

the mean SST at the mooring ($25.63 \pm 0.09^\circ\text{C}$) is significantly higher than in 2006, 2007 and 2009. This is similar to what is observed at the equator. The SST minimum is in September compared to August at the equator with the exception of 2008 when the minimum was in September. This is probably due to the time delay of the cold tongue to reach the mooring. Overall, the SST at the mooring is higher than at the equator because it is not located in the core of the equatorial upwelling and because the cold tongue mixes with warmer water during its westward propagation.

Figure 3 shows the $f\text{CO}_2$, SST, SSS recorded at the mooring as well as $f\text{CO}_2$ calculated at a constant temperature of 25.5°C . The longest time series obtained with the CO_2 sensor is in 2007 with data from January to October (Fig. 3). The warm and cold periods observed at the equator are evidenced in the time series with a mean SST of $27.84 \pm 0.35^\circ\text{C}$ between March and May 2007 and a cooler period with a mean SST of $24.53 \pm 0.6^\circ\text{C}$ between July and October. As previously noticed, at 6°S , 10°W the cooler period is slightly delayed compared to the equator, which is due to the way the cold tongue is advected. Sudden SST decreases are observed on the time series as shown for the 27 August 2006 (arrow on Fig. 3a) and for the 25 August 2009 (arrow on Fig. 3g). This is explained by strips of cooler water located north of the mooring and reaching the mooring (Figs 2a and d). The SST decreases are associated with a salinity decrease (Figs 3b and h). At the mooring, the impact of the cold tongue is characterized by a decrease of salinity because at this location evaporation exceeds precipitation. Therefore, during the warm period the SSS is higher than at the equator. From January to

May 2007, a mean salinity of 36.03 is calculated at 6°S , 10°W while at the equator, the SSS is 35.2 using the SSS recorded at the PIRATA mooring at 0° , 10°W . The salinity decrease is used to detect the arrival of the cold tongue at 6°S , 10°W . The end of the cold tongue period is approximately indicated by the warming of the surface water. The shaded area indicates the main period when the mooring is affected by the cold tongue (Fig. 3).

3.2. Seasonal variability

In 2007, when data are available throughout the year, high $f\text{CO}_2$ values ($431 \pm 6 \mu\text{atm}$) are observed from November to March and lower values from May to August ($397 \pm 19 \mu\text{atm}$). In May–June, $f\text{CO}_2$ is minimum with values close to atmospheric $f\text{CO}_2$ (Fig. 3). To remove the SST effect, $f\text{CO}_2$ is computed at a constant SST of 25.5°C , using the relationship of Takahashi et al. (1993), and is referred as $(f\text{CO}_2)_T$. One striking feature of the $(f\text{CO}_2)_T$ variability is the decrease observed from January to May 2007 (Fig. 3d). Using alkalinity estimated from salinity and $f\text{CO}_2$, DIC can be calculated. This decrease of $(f\text{CO}_2)_T$ corresponds to a decrease of $30 \mu\text{mol kg}^{-1}$ in DIC. It is mostly balanced by a loss of CO_2 by air–sea exchange (estimated to be about $20 \mu\text{mol kg}^{-1}$).

In June–July, the upwelling starts to develop and cold water appears associated with high $f\text{CO}_2$ and lower salinities. For example, between 27 August 2006 and 31 August 2006, $f\text{CO}_2$ increases from 400 to $447 \mu\text{atm}$, and this increase is associated with a decrease in salinity and to a lesser extent in SST. The

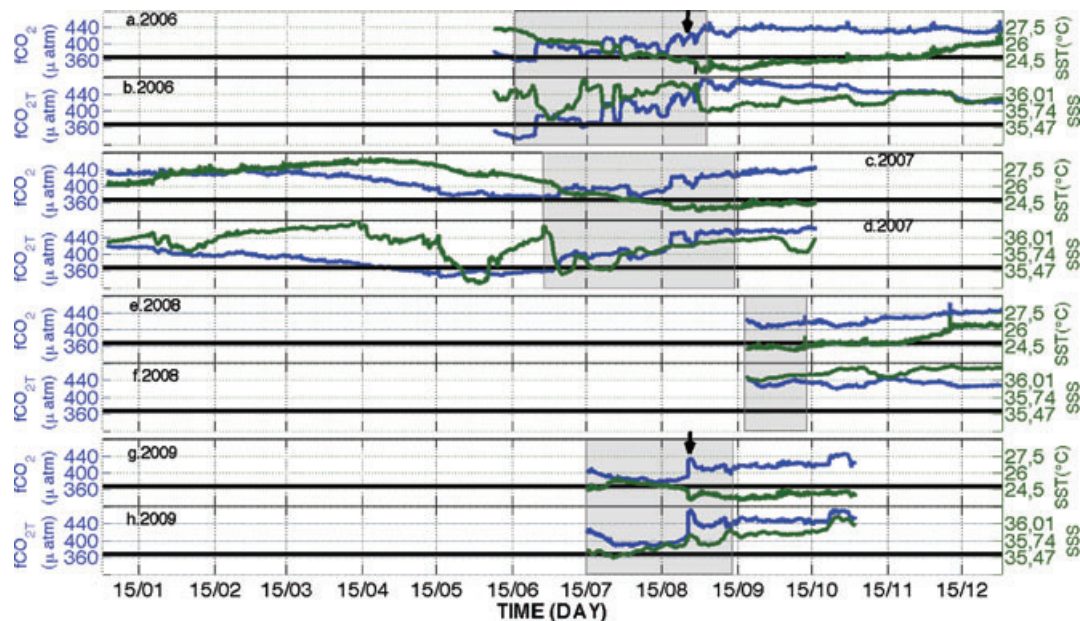


Fig. 3. Time-variability of $f\text{CO}_2$ and SST, $f\text{CO}_2$ at a constant temperature of 25.5°C ($f\text{CO}_2)_T$, and SSS for (a), (b) 2006, (c), (d) 2007, (e), (f) 2008 and (g), (h) 2009. The shaded area corresponds to the period of the impact of the cold tongue at the mooring site. The black arrow corresponds to (a) 27 August 2006 and (g) 25 August 2009. The dashed line represents the mean value of atmospheric $f\text{CO}_2$.

mooring is located in a very dynamical region where patches of warm and cold waters alternate and are responsible for the variability of $f\text{CO}_2$. High $f\text{CO}_2$ values measured in the cold tongue and are maintained by high SST during the warm season. The $f\text{CO}_2$ values are similar to those found in equatorial upwelling regions. For example, Bakker et al. (2001) measured $f\text{CO}_2$ values of 450 μatm in the equatorial Atlantic with a CARIOCA sensor deployed during the upwelling season. In coastal upwelling systems, $f\text{CO}_2$ are much higher with values higher than 600 μatm (Lefèvre, 2009).

Using all the data recorded between June and September, the following $f\text{CO}_2$ -SST relationship is obtained:

$$f\text{CO}_2 = -15.4(\pm 1.08) \times \text{SST} + 785(\pm 16.7) \quad r^2 = 0.76. \quad (3)$$

The predicted error on $f\text{CO}_2$ is $\pm 10 \mu\text{atm}$. This relationship is in good agreement with the one determined for June to September 2006 by Lefèvre et al. (2008) with a slope of $-17.08 \mu\text{atm} (\text{°C})^{-1}$ (Fig. 4). The negative slope characterizes the dominance of the upwelling process with cold temperatures associated with high $f\text{CO}_2$, and is in opposition to the slope of $4.23\% (\text{°C})^{-1}$ due to the thermodynamic effect. The impact of the cold tongue seems to be variable depending on the strength of the upwelling and the ocean circulation. In 2009 for a given temperature, lower $f\text{CO}_2$ values are measured compared to 2006 (Fig. 4). As the mooring is not directly influenced by the upwelling, the data are scattered and some warming effect is visible for temperatures between 23.5 and 24.5 °C with an increase of $f\text{CO}_2$ associated with this warming in 2006 and 2007.

As expected, the increase of $f\text{CO}_2$ due to the propagation of the cold tongue corresponds to an increase of DIC and a

relationship between DIC and SST can be determined

$$\text{DIC} = -17.3(\pm 2) \times \text{SST} + 2468(\pm 16) \quad r^2 = 0.84. \quad (4)$$

The error on predicted DIC is $\pm 12 \mu\text{mol kg}^{-1}$. This relationship is in good agreement with the relationship determined by Lefèvre et al. (2008) who found a slope of $-17.1 \mu\text{mol kg}^{-1} (\text{°C})^{-1}$. The fit is better with DIC than with $f\text{CO}_2$ as there is no warming effect with DIC.

The seasonal amplitude of $f\text{CO}_2$ is quite low ($34 \pm 12 \mu\text{atm}$) compared to other sites in the Atlantic, such as BATS where the seasonal change is 90–100 μatm (Bates et al., 1996) and 60–80 μatm for ESTOC (González-Dávila et al., 2003). Most of the amplitude of $f\text{CO}_2$ at BATS and ESTOC is explained by the seasonal cycle of SST where the temperature varies between 8–10 °C at BATS and 4–6 °C at ESTOC with a minimum in February–March and a maximum in September–October. At CARIACO, high SST are observed in August–October and are associated with high $f\text{CO}_2$. The lowest SSTs are in February–March but they are caused by the coastal upwelling and are associated with low $f\text{CO}_2$ due to the high productivity (Astor et al., 2003, 2005). At PIRATA, the SST amplitude is about 3 °C between the warm season and the cold season. As it is located in the southern hemisphere, the SST maximum is observed in March–April and is associated with high $f\text{CO}_2$. The SST minimum occurs during the cold season, in August–September, and is also associated with high $f\text{CO}_2$ due to the propagation of the cold tongue. High $f\text{CO}_2$ are measured during the cold season and are maintained during the warm season by high temperatures. Low $f\text{CO}_2$ are observed in May–June before the propagation of the cold tongue.

In order to determine the relative importance of the CO₂ air–sea flux, the upwelling, the biological activity and the mixing

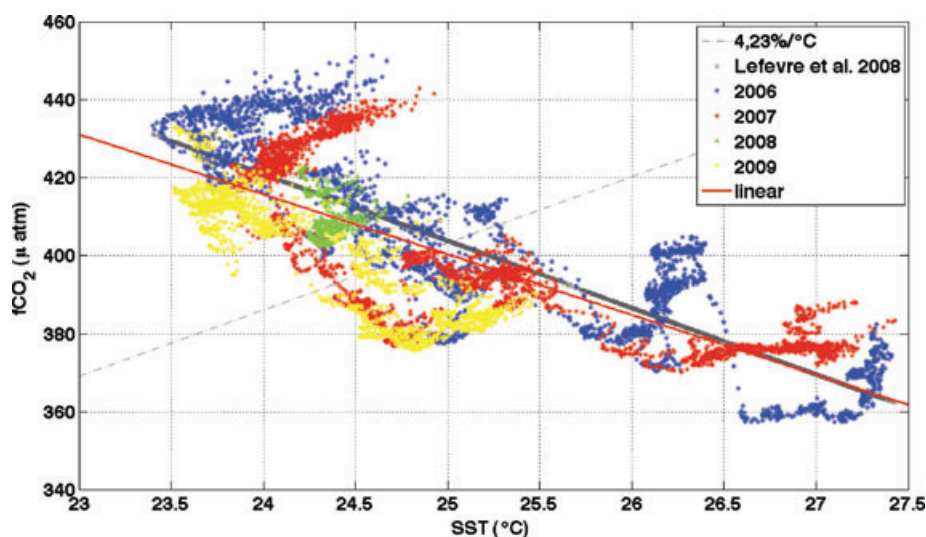


Fig. 4. Relationship between $f\text{CO}_2$ and SST using the mooring data from June to September for each year. The solid line corresponds to the relationship of Lefèvre et al. (2008).

processes at the mooring, monthly DIC variations are calculated. The total DIC variation (ΔDIC) is calculated as the difference between the last and the first day of 1 month and is expressed as follows:

$$\Delta\text{DIC} = \Delta\text{DIC}_{\text{flux}} + \Delta\text{DIC}_{\text{up}} + \Delta\text{DIC}_{\text{other}}, \quad (5)$$

where $\Delta\text{DIC}_{\text{flux}}$ is the variation of DIC due to air–sea exchange. It is calculated by

$$\Delta\text{DIC}_{\text{flux}} = \frac{F_{\text{CO}_2}}{\rho h}, \quad (6)$$

where F_{CO_2} is the monthly CO_2 flux, ρ is the density of seawater and h is the mixed layer depth calculated with Argo floats. The changes of DIC due to the upwelling ($\Delta\text{DIC}_{\text{up}}$) are estimated using eq. (4), with the difference of the mean SST between the last and the first day of each month. $\Delta\text{DIC}_{\text{up}}$ is computed between June and September when SST decreases. As this relationship includes the flux component, the flux term is subtracted from the upwelling component. The $\Delta\text{DIC}_{\text{other}}$ corresponds to the residual term and represents the combined effects of advection, biological activity and vertical mixing. The different components are plotted for each month (Fig. 5). Positive DIC variations correspond to a supply of DIC from the beginning to the end of the month while negative values correspond to a loss. Three phases of DIC variability can be observed with large positive changes during the cold tongue period (June–September), low variability of DIC from September to December and large negative changes from January to March. During the cold tongue period, the $\Delta\text{DIC}_{\text{up}}$ term explains more than 80% of the DIC variation. The losses by outgassing are relatively small with an average, using all the

data, of $2.6 \mu\text{mol kg}^{-1}$, compared to the $14 \mu\text{mol kg}^{-1}$ supplied by the cold tongue and the residuals of $11 \mu\text{mol kg}^{-1}$. Outside the cold tongue period, the air–sea flux contributes to about 6% of the DIC losses on average. This is of the same order of magnitude as the DIC changes explained by air–sea exchange (3–10%) at ESTOC, between October and March. Nevertheless, the flux at 6°S , 10°W contributes to decrease DIC compared to ESTOC (González-Dávila et al., 2003).

After the upwelling season, for example in September 2008, the changes in DIC are lower than $10 \mu\text{mol kg}^{-1}$. The lowest DIC variability is observed from September to December. As the contribution of the CO_2 flux is small, most of the variations are explained by mixing with water masses and/or biological activity.

Before the cold tongue period, from March to June 2007, ΔDIC show large negative changes. The DIC decrease is associated with an increase in the remaining component (biological activity/mixing processes). The correlation between DIC and SSS suggests that the DIC variability is explained mostly by the mixing of water masses. Over this period, a relationship between DIC and SSS can be determined

$$\text{DIC} = 73.7(\pm 1.6) \times \text{SSS} - 627(\pm 4.5) \quad r^2 = 0.94. \quad (7)$$

The error on predicted DIC is about $9 \mu\text{mol kg}^{-1}$. The relationship between $f\text{CO}_2$ and SSS is not so strong ($r^2 = 0.87$) as $f\text{CO}_2$ is also affected by SST and air–sea exchange. The large negative variability of DIC is mainly explained by advection.

At ESTOC, between March and October, the DIC changes are explained by net organic production, and advection was negligible compared to the PIRATA mooring where advection is

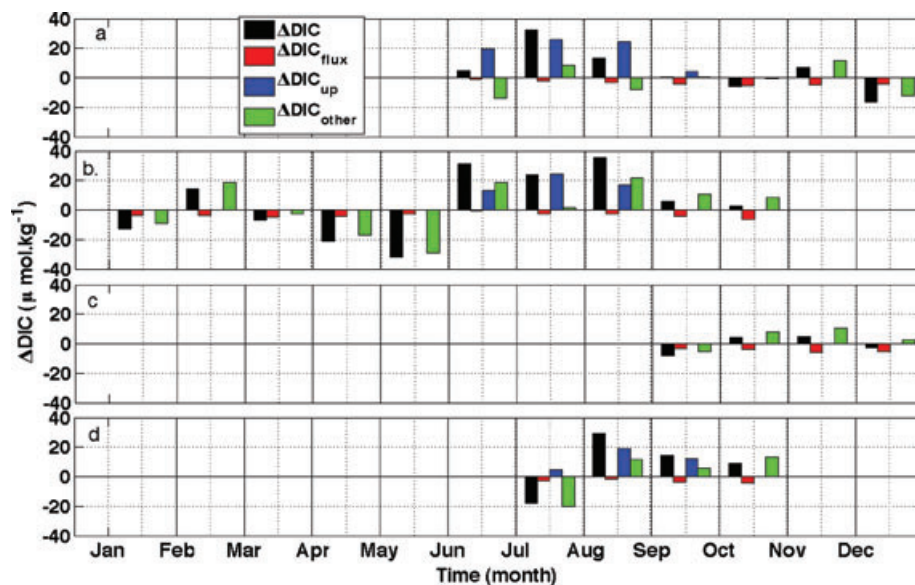


Fig. 5. Monthly variations of DIC (in $\mu\text{mol kg}^{-1}$) calculated as the difference between the last day and the first day of the month with contributions of the air–sea exchange ($\Delta\text{DIC}_{\text{flux}}$), the cold tongue impact ($\Delta\text{DIC}_{\text{up}}$), and the remaining processes ($\Delta\text{DIC}_{\text{other}}$) for (a) 2006, (b) 2007, (c) 2008 and (d) 2009.

responsible for most of the DIC variations between March and October (González-Dávila et al., 2003).

3.3. Year to year variability

The $f\text{CO}_2$ variability at the mooring during the cold tongue period depends on the strength of the equatorial and coastal upwellings, and on the westward propagation of the cold tongue. However, on monthly average, $f\text{CO}_2$ is not significantly different from one year to another for the months of June, July and August. In September, higher $f\text{CO}_2$ values are measured in 2006 ($434 \pm 7 \mu\text{atm}$) and 2007 ($430 \pm 5 \mu\text{atm}$) compared to 2008 ($409 \pm 5 \mu\text{atm}$) and 2009 ($412 \pm 5 \mu\text{atm}$).

In addition to the impact of the cold tongue on the mean $f\text{CO}_2$ values measured at 6°S , 10°W , the time series is characterized by high variability due to intrusions of cooler water. Overall, the SST distribution is similar from one year to another. During the July–December period, when several years of data are available, the SST follows the same pattern with a decrease in June–July, followed by a minimum in September and an increase towards December. It is more difficult to detect a repeated pattern on the $f\text{CO}_2$ and SSS distributions as they exhibit significant decreases and increases.

Previous estimates of $f\text{CO}_2$ have been reported for the eastern tropical Atlantic and can be compared to the data recorded at the mooring. As the $f\text{CO}_2$ variability can be affected by the different oceanic conditions, $f\text{CO}_2$ is corrected to a mean SST of 27°C according to the relationship given by Takahashi et al. (1993). The comparison is done for the year 2007 (Fig. 6) as $f\text{CO}_2$ data are available throughout the year.

In 1984, during the FOCAL 6 cruise, $f\text{CO}_2$ was measured during boreal winter, at 3°S – 5°S , 4°W (Andrié et al., 1986).

The atmospheric $f\text{CO}_2$ increased by $37 \mu\text{atm}$ and oceanic $f\text{CO}_2$ by $29 \pm 11 \mu\text{atm}$ between 1984 and 2007 (the uncertainty of the oceanic increase of $11 \mu\text{atm}$ has been computed from the sum of the variances of $f\text{CO}_2$ in 1984 and 2007). The increase of seawater $f\text{CO}_2$ ($1.3 \mu\text{atm yr}^{-1}$) is quite similar to the atmospheric increase of $1.6 \mu\text{atm yr}^{-1}$.

Ten years later, in March 1993, Oudot et al. (1995) revisited the 4°W section. Between 1993 and 2007, the seawater $f\text{CO}_2$ increases by 30 ± 11 and $24 \mu\text{atm}$ in the atmosphere. They reported an increase between 1984 and 1993 after correcting from temperature [$1.3\% (\text{C}^\circ)^{-1}$] and salinity [$44 \mu\text{atm} (\text{psu})^{-1}$] effects. However, these relationships are not valid at 6°S , 10°W and could not be applied.

Further west of the mooring, near 15°W , the $f\text{CO}_2$ was measured in April and July 1995 on board the RMS St Helena (Lefèvre et al., 1998). Between 4°S and 7°S , a lower $f\text{CO}_2$ is measured in April (warm season) compared to July (cold season). From 1995 to 2007, atmospheric $f\text{CO}_2$ increased by $23 \mu\text{atm}$ in April and $18 \mu\text{atm}$ in July whereas seawater $f\text{CO}_2$ increased by $28 \pm 10 \mu\text{atm}$ in April and $42 \pm 14 \mu\text{atm}$ in July.

Seawater $f\text{CO}_2$ at the mooring is higher in 2007 than during previous cruises carried out in the area. With the exception of the FOCAL 6 cruise where atmospheric and oceanic $f\text{CO}_2$ increase at a similar rate, the comparison of previous measurements with the 2007 data shows that seawater $f\text{CO}_2$ increases faster than atmospheric $f\text{CO}_2$. The highest seawater $f\text{CO}_2$ increase is observed in July when the cold tongue reaches the mooring. This might be due to the high $f\text{CO}_2$ variability occurring at this time of the year. The comparison is probably more robust during the warm period. However, as this region is highly dynamic it is difficult to assess the trend of seawater $f\text{CO}_2$ from the different cruises made in this region. The long term monitoring of $f\text{CO}_2$ at

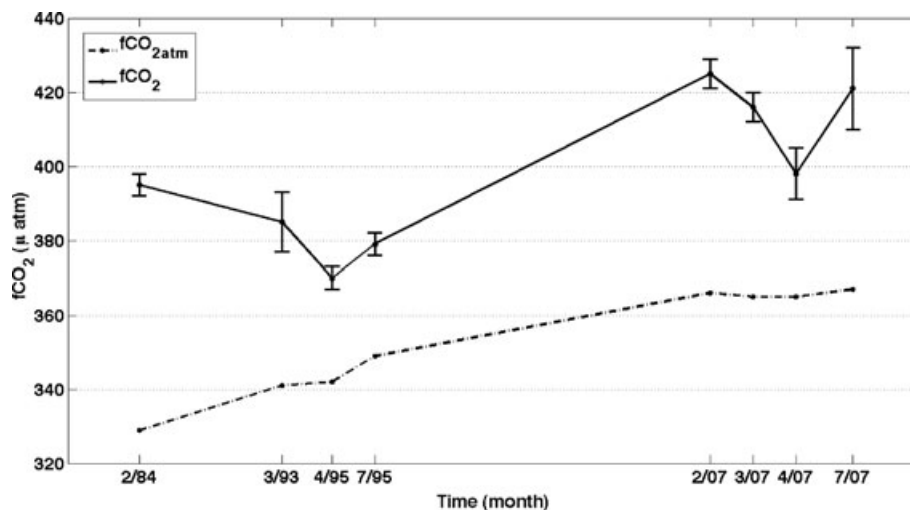


Fig. 6. Mean seawater $f\text{CO}_2$ corrected to an SST of 27°C using the relationship of Takahashi et al. (1993) as a function of time (month/year). The data come the FOCAL 6 cruise in 1984 (Andrié et al., 1986), the Cither 1 cruise in 1993 (Oudot et al., 1995), the St Helena cruises in 1995 (Lefèvre et al., 1998) and the 2007 data at 6°S , 10°W . The dashed line corresponds to the mean atmospheric $f\text{CO}_2$ ($f\text{CO}_{2\text{atm}}$) measured during the different cruises.

the PIRATA station should help to determine the rate of increase of seawater $f\text{CO}_2$ more precisely.

3.4. High frequency variability

Superimposed on the seasonal variability, the time series shows high frequency variability. In order to highlight the diurnal cycle, a wavelet study was done (Fig. 7). The wavelet modulus represents the importance of the frequency observed. It is maximum around 24 h, which corresponds to the diurnal cycle (Fig. 7.1). During the cold tongue period, the diurnal cycle is less often observed, as shown by the wavelet modulus (Figs 7a–c). However, it dominates from January to May and after September 2008 and 2009.

The most significant scale of variability in $f\text{CO}_2$ between 2006 and 2007 has a period of 1 d, and is clearly depicted in the wavelet analysis, as a significant peak in the mean wavelet power spectrum (Fig. 7.2) for a period lower or equal to 5 d. The amplitude of the $f\text{CO}_2$ diurnal cycle is usually very small (less than a few micro atmospheres) although a maximum of 23.2 μatm was observed in December 2006.

Strong SST and SSS variations are observed when the cold tongue propagates and reaches the mooring so that the diurnal cycle is masked by this large signal. During the warm season, oceanic conditions are more stable and $f\text{CO}_2$ varies with SST. From January to May 2007, ten periods of thermodynamical events are observed with an increase of $f\text{CO}_2$ close to $4.23\% (\text{°C})^{-1}$ over a period from 2 to 10 d (4 d on average). From September to December 2006 and 2008, six periods are observed whereas, during the cold tongue period, two periods of

thermodynamical events can be detected. The wavelet analysis also captures 1-d variability that can be due to changes of water masses occurring during that period. In this case, no diurnal cycle is observed. This 1-d variability is observed mainly during the cold tongue period when changes of water masses occur more frequently.

However, a few periods show no correlation between $f\text{CO}_2$ and SST despite the presence of the diurnal cycle of SST. Most of these periods are observed after and during the upwelling season. We consider that if the following conditions are observed, the variation of DIC can only due to the biological variability. The TA must remain fairly constant to neglect the variation of DIC due to advection. This condition is met when the change of TA is less than $\pm 1 \mu\text{mol kg}^{-1}$, which corresponds to a change of SSS less than 0.02. When the DIC is maximum at sunrise and minimum at sunset, if we observed a decrease of DIC over a given period, the variability of DIC must be caused by biological activity. A few periods with these criteria have been identified (Fig. 8a). Surprisingly, most of them occur during the cold tongue period.

Under these conditions, a NCP can be estimated following the method of Boutin and Merlivat (2009) and using the following equation:

$$\text{NCP} = \frac{\Delta C}{\Delta t} + \frac{F}{\rho h}, \quad (8)$$

where $\Delta C/\Delta t$ is the decrease of maximum DIC at sunrise over a period of several days, F is the air–sea CO_2 flux, ρ is the density of seawater and h is the mixed layer depth. The mixed layer depth was estimated with the ARGO profiler and compared

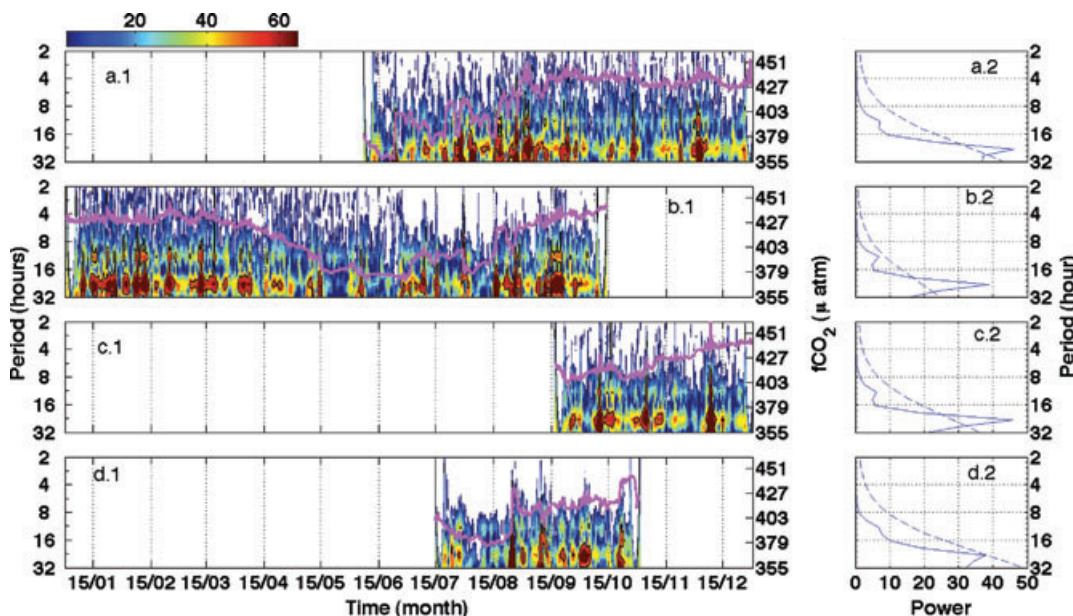


Fig. 7. The modulus of the wavelet transform, using the Morlet wavelet, is shown for $f\text{CO}_2$ in (a.1) 2006, (b.1) 2007, (c.1) 2008, (d.1) 2009. The $f\text{CO}_2$ data are also shown on these plots (solid line). The left-hand panels correspond to the mean power of the global spectrum (solid curve) with the 95% significance level (dashed curve) for (a.2) 2006, (b.2) 2007, (c.2) 2008 and (c.2) 2009.

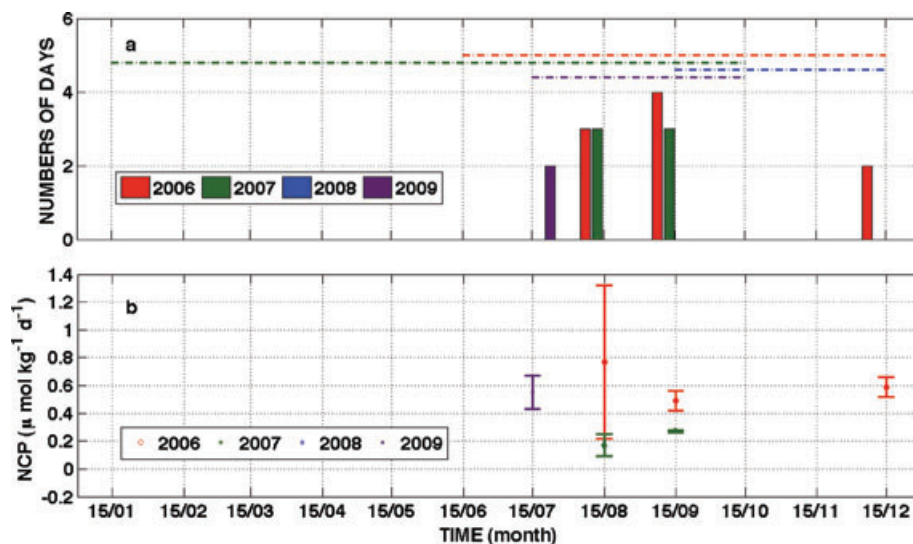


Fig. 8. (a) Number of days from January to December when biological events are observed. The dash-dotted lines at the top of figure indicate the periods with available data. (b) estimates of net community production (in $\mu\text{mol kg}^{-1} \text{d}^{-1}$).

with mooring data at several depths. The NCP ranges from 0.17 to $0.77 \mu\text{mol kg}^{-1} \text{d}^{-1}$ (Fig. 8b).

NCP integrated over the mixed layer is computed for each biological event, and ranges from 9 to $41 \text{ mmol m}^{-2} \text{d}^{-1}$.

These values are in good agreement with previous estimates. A first study was conducted during the Equalant cruise in 1963 where the oxygen saturation was used to estimate primary production (Voituriez and Herbland, 1982). They obtained an estimate of Net Primary Production which is equivalent to an NCP of $0.76 \mu\text{mol kg}^{-1} \text{d}^{-1}$ assuming an autotrophic regime for the region 6°S , 10°W in August 1963. This is close to our estimations of $0.77 \mu\text{mol kg}^{-1} \text{d}^{-1}$ in August 2006 and $0.17 \mu\text{mol kg}^{-1} \text{d}^{-1}$ in August 2007. Another cruise took place in December 1971, between 0°N and 11°S at the meridian 4°W , where Dufour and Stretta (1973) measured primary production which, converted to NCP, gives an estimate ranging from 0.24 to $0.96 \mu\text{mol kg}^{-1}$ that compares well with our estimate of $0.59 \mu\text{mol kg}^{-1}$ for December 2006.

3.5. Air-sea CO₂ flux

The monthly air-sea CO₂ flux follows the $f\text{CO}_2$ pattern as higher values are observed in the boreal winter and a decrease is found in May–June before the upwelling season (Fig. 9). The air-sea CO₂ flux reaches its minimum in June with a mean value of $0.56 \pm 0.61 \text{ mol m}^{-2} \text{yr}^{-1}$ calculated using the 2006 and 2007 data. The maximum is reached in November with a mean of $3.21 \pm 0.8 \text{ mol m}^{-2} \text{yr}^{-1}$ calculated with 2006 and 2008 data. A source of CO₂ is observed throughout the year. In 2007, measurements are available for almost a complete year. On annual average for 2007, the CO₂ flux is $2.1 \pm 0.69 \text{ mol m}^{-2} \text{yr}^{-1}$. It is of the same order of magnitude as the CO₂ flux of $2.8 \pm 3.6 \text{ mol m}^{-2} \text{yr}^{-1}$ measured at the CARIACO site from 1996 to 2000. However,

the CO₂ variability at PIRATA is lower than at CARIACO as it is not directly influenced by the upwelling unlike CARIACO (Astor et al., 2003).

The air-sea CO₂ flux is computed with daily wind speed because hourly wind speed was not available for 2008 and 2009. However, the use of daily wind speed did not affect the estimate the annual CO₂ flux by more than 3.5%. The estimation of the error on the CO₂ flux using measurements sampled once a day is as well very low, less than 5%. This is in agreement with a previous study at BATS (Bates et al., 1998) showing that the sampling frequency affects the estimates of the CO₂ flux by no more than 5–10%.

For the tropical Atlantic between 14°S and 14°N , the source of CO₂ is $0.46 \text{ mol m}^{-2} \text{yr}^{-1}$ (Takahashi et al., 2009) which is significantly lower than our value at 6°S , 10°W .

In order to compare the CO₂ flux at the mooring with the climatology of Takahashi et al. (2009) built for the reference year 2000, we used the $\Delta p\text{CO}_2$ provided by the climatology in the box $4\text{--}8^{\circ}\text{S}$ and $7.5\text{--}12.5^{\circ}\text{W}$. We calculated the CO₂ flux with the gas exchange coefficient used for our CO₂ flux. The climatological CO₂ flux is lower than the estimates at the mooring (Fig. 9). The annual mean is $0.79 \text{ mol m}^{-2} \text{yr}^{-1}$ compared to our estimate of $2.1 \pm 0.69 \text{ mol m}^{-2} \text{yr}^{-1}$. For the box $4\text{--}8^{\circ}\text{S}$, $7.5\text{--}12.5^{\circ}\text{W}$, this corresponds to a flux of 0.08 PgC yr^{-1} for the climatological value compared to our estimate of 0.22 PgC yr^{-1} for the year 2007. Possible explanations for this discrepancy are the coarse resolution of the climatology built on a 4° of latitude by 5° of longitude grid and the lack of data in this region. In addition, the comparison between the CO₂ flux and the climatology for the year 2000 assumes that $\Delta f\text{CO}_2$ is constant over the years. If seawater $f\text{CO}_2$ increases faster than the atmospheric increase, the CO₂ flux calculated from 2006 to 2009 should be higher than the flux in 2000. However, the time series is still too short

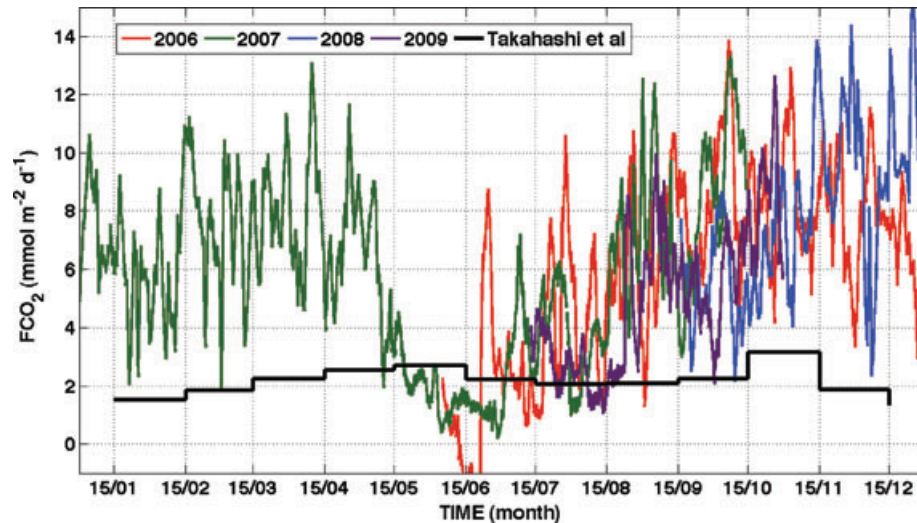


Fig. 9. The daily air–sea CO_2 flux (in $\text{mmol m}^{-2} \text{d}^{-1}$) at 6°S , 10°W for the years 2006, 2007, 2008 and 2009. In black, the Takahashi et al.'s climatology (2009).

to detect any trend. The comparison between previous cruises seems to indicate a higher seawater $f\text{CO}_2$ increase compared to the atmospheric increase. However, the dynamics of this region makes the comparison difficult and a longer time series is required to draw a conclusion. The CO_2 flux at 6°S , 10°W is unlikely to be representative of the equatorial Atlantic because a north–south gradient occurs between the NECC and the SEC and lower $f\text{CO}_2$ are observed in the NECC. If the flux at 6°S , 10°W were representative of the SEC system then the source of CO_2 in this area would be significantly underestimated.

4. Summary

A CARIOCA sensor has been installed on the PIRATA mooring at 6°S , 10°W and has recorded hourly $f\text{CO}_2$ since June 2006. Although not directly located in the upwelling area, the mooring is affected by the spreading of the cold tongue during the upwelling season. Patches of cold water are advected, which explains the high variability of the $f\text{CO}_2$ distribution. The site is strongly affected by advection, even before the propagation of the cold tongue. A wavelet analysis highlights the high frequency variability at 24 h. Diurnal cycles occur mainly during the warm season over 2–10 d, with an average of 4 d. The dominant process controlling this variability is the thermodynamical effect with an $f\text{CO}_2$ increase close to the relationship of $4.23\% (\text{ }^\circ\text{C})^{-1}$. Short periods dominated by biological activity are also identified. During these periods, a NCP is calculated from the decrease of DIC over the whole period. Estimates of NCP range from 9 to $41 \text{ mmol m}^{-2} \text{d}^{-1}$ and are in agreement with previous estimates.

In 2007, when almost a complete year of data is available, a source of CO_2 is observed throughout the year with an annual average of $2.1 \pm 0.69 \text{ mol m}^{-2} \text{yr}^{-1}$. The variability of the CO_2

flux is characterized by a minimum in June and a maximum in November. This source corresponds to a flux of 0.22 PgC yr^{-1} for the $4\text{--}8^\circ\text{S}$ and $7.5\text{--}12.5^\circ\text{W}$ box. Although this estimate is unlikely to be representative of the equatorial Atlantic, because of the north–south gradient of $f\text{CO}_2$, it might be representative of the southeastern Atlantic. More data in the South Atlantic would help in determining whether the source of CO_2 in this region is currently underestimated.

In addition, pursuing the monitoring at 6°S , 10°W is required to assess whether the source of CO_2 is increasing with time. A comparison of seawater $f\text{CO}_2$ with previous cruises suggests that seawater $f\text{CO}_2$ increases at a faster rate than atmospheric $f\text{CO}_2$ in recent years.

5. Acknowledgments

We thank Liliane Merlivat and Leticia Barbero for helpful discussions. We thank Marion Leduc Leballeur for her help with Matlab. This work is funded by the European Integrated Project CARBOOCEAN (contract 511176–2). TMI data are produced by Remote Sensing Systems and sponsored by the NASA Earth Science and REASoN DISCOVER project. They are available at <http://www.remsss.com>. ARGO is a pilot program of the Global Ocean Observing System. The data were collected and made freely available by the international Argo Project and the national programs that contribute to it (<http://www.argo.net>).

References

- Andrié, C., Oudot, C., Genthon, C. and Merlivat, L. 1986. CO_2 fluxes in the tropical Atlantic during FOCAL cruises. *J. Geophys. Res.* **91**, 11741–11755.

- Astor, Y., Muller-Karger, F. and Scranton, M. I. 2003. Seasonal and interannual variation in the hydrography of the Cariaco Basin: implications for basin ventilation. *Continental Shelf Res.* **23**, 125–144.
- Astor, Y. M., Scranton, M. I., Muller-Karger, F., Bohrer, R. and Garcia, J. 2005. fCO₂ variability at the CARIACO tropical coastal upwelling Time Series Station. *Mar. Chem.* **97**, 245–261.
- Bakker, D. C., Echeto, J., Boutin, J. and Merlivat, L. 2001. Variability of surface water fCO₂ during seasonal upwelling in the equatorial Atlantic Ocean as observed by a drifting buoy. *J. Geophys. Res.* **106**, 9241–9253.
- Bakker, D. C. E., de Baar, H. J. W. and de Jong, E. 1999. The dependence on temperature and salinity of dissolved inorganic carbon in East Atlantic surface waters. *Mar. Chem.* **65**, 263–280.
- Bakun, A. 1978. Guinea Current upwelling. *Nature* **271**, 147–150.
- Bates, N. R., Michaels, A. F. and Knap, A. H. 1996. Seasonal and interannual variability of oceanic carbon dioxide species at the US JGOFS Bermuda Atlantic Time-series Study (BATS) site. *Deep Sea Res. Part II: Topical Stud. Oceanogr.* **43**, 347–383.
- Bates, N. R., Takahashi, T., Chipman, D. W. and Knap, A. H. 1998. Variability of pCO₂ on diel to seasonal timescales in the Sargasso Sea near Bermuda. *J. Geophys. Res.* **103**, 15567–15585.
- Bates, N. R., Merlivat, L., Beaumont, L. and Pequignot, C. A. 2000. Intercomparison of shipboard and moored CARIOCA buoy seawater fCO₂ measurement in Saragossa Sea. *Mar. Chem.* **72**, 239–255.
- Bindoff, N. L., Willebrand, J., Artale, V., Cazenave, A., Gregory, J. and co-authors. 2007. Observations: oceanic climate change and sea level. In: *Climate Change: The Physical Science Basis. Contribution of working group 1 to the Fourth Assessment Report of the Intergovernmental Panel on Climate Change* (eds S. Solomon, D. Qin, M. Manning, Z. Chen, M. Marquis and co-authors), Cambridge University Press, Cambridge, United Kingdom and New York, NY, USA, 385–432.
- Bourlès, B., Lumpkin, R., Phaden, M. M., Hernandez, F., Nobre, P. and co-authors. 2008. THE PIRATA PROGRAM: history, Accomplishments, and Future Directions. *Bull. Am. Meteorol. Soc.* **89**, 1111–1125.
- Boutin, J. and Merlivat, L. 2009. New in situ estimates of carbon biological production rates in the Southern Ocean from CARIOCA drifter measurements. *Geophys. Res. Lett.* **36**, 1–6.
- Boyer Montégut, C., Madec, G., Fischer, A. S., Lazar, A. and Ludicone, D. 2004. Mixed layer depth over the global ocean: an examination of profile data and a profile-based climatology. *J. Geophys. Res.* **109**, C12003, doi: 10.1029/2004JC002378.
- Byrne, R. H., Degrandpre, M. D., Short, R. T., Martz, T. R., Merlivat, L. and co-authors. 2009. Sensors and systems for in situ observations of marine CO₂ system variables. In: *Proceedings of the OceanObs09*, Venice, Italy, September 21–25, 2009. Available at: <http://www.oceanobs09.net/>.
- Chavez, F. P., Pennington, T. J., Herlien, R., Jannasch, J. H., Thurmond, G. and co-authors. 1997. Moorings and drifters for real-time interdisciplinary oceanography. *Am. Meteorol. Soc.* **14**, 1199–1211.
- Copin-Montégut, C., Bégovic, M. and Merlivat, L. 2004. Variability of the partial pressure of CO₂ on diel to annual time scales in the Northwestern Mediterranean Sea. *Mar. Chem.* **85**, 169–189.
- Dickson, A. and Millero, F. 1987. A comparison of the equilibrium constants for the dissociation of carbonic acid in seawater media. *Deep Sea Res. Part A. Oceanogr. Res. Papers* **34**, 1733–1743.
- Dufour, P. and Stretta, J. M. 1973. Production primaire, biomasse du phytoplancton et du zooplancton dans l'Atlantique tropical sud, le long du méridien 4°W. *Ser. Océanogr.* **11**, 419–429.
- González-Dávila, M., Santana-Casiano, J. M., Rueda, M. J., Llinás, O. and González-Dávila, E. F. 2003. Seasonal and interannual variability of sea-surface carbon dioxide species at the European Station for Time Series in the Ocean at the Canary Islands (ESTOC) between 1996 and 2000. *Global Biogeochem. Cycles* **17**, 1076.
- Hazeleger, W., de Vries, P. and Friocourt, Y. 2003. Sources of the equatorial undercurrent in the Atlantic in a high-resolution ocean model. *J. Phys. Oceanogr.* **33**, 677–693.
- Hood, E. M. and Merlivat, L. 2001. Annual to interannual variations of fCO₂ in the northwestern Mediterranean Sea: high frequency time series data from CARIOCA buoys (1995–1997). *J. Mar. Res.* **59**, 113–131.
- Koffi, U., Lefèvre, N., Kouadio, G. and Boutin, J. 2010. Surface CO₂ parameters and air-sea CO₂ flux distribution in the eastern equatorial Atlantic. *J. Mar. Syst.* **82**, 135–144.
- Körtzinger, A. 2003. A significant CO₂ sink in the tropical Atlantic Ocean associated with the Amazon River plume. *Geophys. Res. Lett.* **30**, 2287.
- Körtzinger, A., Send, U., Wallace, D. W. R., Karstensen, J. and DeGrandpre, M. 2008. Seasonal cycle of O₂ and pCO₂ in the central Labrador Sea: atmospheric, biological, and physical implications. *Global Biogeochem. Cycles* **22**, 1–16.
- Lefèvre, N. 2009. Low CO₂ concentrations in the Gulf of Guinea during the upwelling season in 2006. *Mar. Chem.* **113**, 93–101.
- Lefèvre, N., Ciabini, J. P., Michard, G., Briest, B., Duchaffaut, M. and co-authors. 1993. A new optical sensor for pCO₂ measurement. *Mar. Chem.* **42**, 189–198.
- Lefèvre, N., Moore, G., Aiken, J., Watson, A. and Cooper, D. 1998. Variability of pCO₂ in tropical Atlantic in 1995. *J. Geophys. Res.* **103**, 5623–5634.
- Lefèvre, N., Guillot, A., Beaumont, L. and Danguy, T. 2008. Variability of fCO₂ in the Eastern Tropical Atlantic from a moored buoy. *J. Geophys. Res.* **113**, 1–12.
- Lefèvre, N., Diverres, D. and Gallois, F. 2010. Origin of CO₂ undersaturations in the western tropical Atlantic. *Tellus B*, doi: 10.1111/j.1600-0889.2010.00475.x.
- Leinweber, A., Gruber, N., Fenzel, H., Friedeich, G. E. and Chavez, F. P. 2009. Diurnal carbon cycling in the surface ocean and lower atmosphere of Santa Monica Bay, California. *Geophys. Res. Lett.* **36**, 1–5.
- Merbach, C., Culberson, C. H. and Hawley, J. E. 1973. Measurements of the apparent dissociation constants of carbonic acid in seawater of atmospheric pressure. *Lymnol. Oceanogr.* **18**, 897–907.
- Merlivat, L., Davila, M., Caniaux, G. and Boutin, J. 2009. Mesoscale and diel to monthly variability of CO₂ and carbon fluxes at the ocean surface in the northeastern Atlantic. *J. Geophys. Res.-Oceans* **114**, 1–17.
- Oudot, C., Ternon, J. and Lecomte, J. 1995. Measurements of atmospheric and oceanic CO₂ in the tropical Atlantic: 10 years after the 1982–1984 FOCAL cruises. *Tellus* **47B**, 70–85.
- Sayles, F. L. and Eck, C. 2009. An autonomous instrument for time series analysis of TCO₂ from oceanographic moorings. *Deep Sea Res. Part I: Oceanogr. Res. Papers* **56**, 1590–1603.

- Send, U., Weller, R., Wallace, D., Chavez, F., Lampitt, R. and co-authors. 2009. OceanSITES. In: *Proceedings of the OceanObs09*, Venice, Italy, September 21–25, 2009. Available at: <http://www.oceanobs09.net/>.
- Stramma, L. and Schott, F. 1999. The mean flow field of the tropical Atlantic Ocean. *Deep-sea Res. II* **46**, 279–303.
- Sweeney, C., Gloor, E., Jacobson, A. R., Key, R. M., McKinley, M. and co-authors. 2007. Constraining global air-sea gas exchange for CO₂ with recent bomb ¹⁴C measurements. *Global Biogeochem. Cycles* **21**, 1–10.
- Takahashi, T., Olafsson, J., Goddard, J. G., Chipman, D. W. and Sutherland, S. C. 1993. Seasonal variation of CO₂ and nutrients in the high-latitude surface oceans: a comparative study. *Global Biogeochem. Cycles* **7**, 843–878.
- Takahashi, T., Sutherland, S. C., Wanninkhof, R., Sweeney, C., Feely, R. A. and co-authors. 2009. Climatological mean and decadal change in surface ocean pCO₂, and net sea–air CO₂ flux over the global oceans. *Deep-Sea Res. Part II* **56**, 554–577.
- Ternon, J., Oudot, C., Dessier, A. and Diverres, D. 2000. A seasonal tropical sink for atmospheric CO₂ in the Atlantic Ocean: the role of the Amazon River discharge. *Mar. Chem.* **68**, 183–201.
- Torrence, C. and Compo, G. P. 1998. A practical guide to wavelet analysis. *Bull. Am. Meteorol. Soc.* **79**, 61–78.
- Voituriez, B. and Herbland, A. 1979. The use of the salinity maximum of the Equatorial Undercurrent for estimating nutrient enrichment and primary production in the Gulf of Guinea. *Deep Sea Res. Part A. Oceanogr. Res. Papers* **26**, 77–83.
- Voituriez, B. and Herbland, A. 1982. Primary production in the Tropical Atlantic ocean mapped from oxygen values of equalant 1 and 2 (1963). *Bull. Mar. Sci.* **31**, 853–863.
- Weiss, R. F. 1974. CO₂ in water and seawater: the solubility of a non ideal gas. *Mar. Chem.* **2**, 203–215.
- Weiss, R. F. and Price, B. A. 1980. Nitrous oxide solubility of a non ideal gas. *Mar. Chem.* **8**, 347–359.